Identification of eQTL and sQTL associated with meat quality in beef

Joel David Leal Gutierrez (joelleal@ufl.edu)
University of Florida https://orcid.org/0000-0002-2811-5390
Mauricio A. Elzo
University of Florida
Raluca G. Mateescu
University of Florida

Research article

Keywords: Cis effect, DE gene, expression master regulator, meat quality, splicing master regulator and trans effect

Posted Date: September 30th, 2019

DOI: https://doi.org/10.21203/rs.2.15326/v1

Version of Record: A version of this preprint was published on January 30th, 2020. See the published version at https://doi.org/10.1186/s12864-020-6520-5.

Abstract

Background: Transcription has a substantial genetic control and genetic dissection of gene expression could help us understand the genetic architecture of complex phenotypes such as meat quality in cattle.

Results: A total of 80 steers were selected for phenotyping, genotyping and RNA-seq evaluation. A panel of traits related to meat quality were recorded. Information on 112,042 SNPs and expression data on 8,588 autosomal genes and 87,770 exons from 8,467 genes were included in an expression and splicing quantitative trait loci (QTL) mapping (eQTL and sQTL, respectively). Expression of 1,352 genes was previously identified as associated with meat quality traits using a gene, exon and isoform differential expression (DE) analysis. The R package Matrix eQTL was used to perform the QTL mapping using linear regression. The identified QTLs were classified as cis or trans using 1 Mb as maximum distance between the associated SNP and the gene. Polymorphisms associated with expression of at least 20 genes, and splicing of at least 20 exons were considered QTL hot spots. A total of 8,377 eQTLs were identified, including 75.6% trans, 10.4% cis, 12.5% DE trans and 1.5% DE cis; 11,929 sQTLs were uncovered: 66.1% trans, 16.9% DE trans, 14% cis and 3% DE cis. Twenty seven expression master regulators and 13 splicing master regulators were identified and were classified as membrane associated or cytoskeletal proteins, transcription factors or DNA methylases These genes could control expression of other genes through cell signaling or by a direct transcriptional activation/repression mechanism. The ZNF804A, ALAD, OR13F1 and ENSBTAG00000000336 genes were identified as both expression and splicing master regulators.

Conclusion: In the present analysis, we show that eQTL and sQTL mapping makes possible positional identification of gene and isoform expression regulators. Additionally, this mapping provides new insight into the regulatory network architecture in longissimus dorsi muscle in an Angus-Brahman multibreed population.

Background

Little knowledge exists about transcription variation patterns across the genome as well as how much of this variability is under genetic control. Regulatory variation has been proposed as a primary factor associated with phenotypic variability [1,2]. Based on some estimates, gene expression can be classified as medium-highly heritable [1]. Since transcription has a substantial genetic control, genetic dissection of gene expression is useful for understanding the genetic architecture of complex phenotypes such as meat quality. Toward this goal, eQTL and sQTL mapping analyses allow for uncovering specific genomic regions associated with transcription, which are further related to phenotypic variation.

eQTL and sQTL can be classified into cis (local) and trans (distant) effects. A large fraction of human genes are enriched for cis regulation and in some cases, the cis effect is able to explain trans effects located in the harboring gene. Pierce et al. uncovered 434 trans eQTLs in mononuclear cells and 189 of these genes also harbor cis eQTLs [2]. Out of the 189 identified genes, 39 showed a significant trans effect attenuation after adjusting for cis mediation. Therefore, cis regulation could explain a substantial proportion of variability associated with trans effects and their associated complex phenotypes, at least at molecular level [2]. On the other hand, trans regulation is more difficult to identify and explain [2], but it allows for the identification of “hot spots” which are also known as master regulators with transcriptional control over a suite of genes usually

involved in the same biological pathway [3]. Therefore, trans regulation might be suggested as the primary factor determining phenotypic variation in complex phenotypes [1] such as meat quality in cattle.

Variability at the DNA level which is usually interrogated through genome-wide association studies has been proven a very useful tool for animal selection and breeding programs. However, eQTL and sQTL mapping connects variability at gene expression level to DNA variability and this information can be used to formulate and validate hypotheses about the biology of complex traits such as meat quality. Both eQTL and sQTL analyses allow for the positional identification of gene and isoform expression regulators and provide insights into the regulatory network architecture [4] of complex traits.

The objectives of the present research were: 1) to perform eQTL and sQTL mapping analyses in *longissimus dorsi* muscle focused on meat quality; 2) to uncover genes with highly significant cis effects; 3) to identify expression and splicing hot spots; and 4) to uncover genes whose expression is influenced by multiple genomic regions (multigenic effects).

Result

On average, 39.8 million paired reads per sample were available for mapping, and out of these, 34.9 million high-quality paired reads were uniquely mapped to the Btau_4.6.1 reference genome. The mean fragment inner distance was equal to 144±64 bps.

2.1. Expression QTL mapping

A total of 8,377 eQTLs were identified in the present population (Figure 1). The most frequently identified types of eQTLs were trans (75.6%) followed by cis (10.4%) (Figure 2A). Only 12.5% of the eQTLs were classified as DE trans and 1.5% as DE cis. The majority of SNP with trans and DE trans effect were associated with expression of only one gene (76.2 and 84.0%, respectively.

2.1.1. Expression cis and DE cis eQTL analysis

A total of 868 cis and 125 DE cis eQTLs were uncovered. SNPs rs110591035 and rs456174577 were cis eQTLs and they were highly associated with expression of LSM2 Homolog, U6 Small Nuclear RNA And MRNA Degradation Associated (LSM2) (p-value = 5.8x10-9) and Sterol O-Acyltransferase 1 (SOAT1) (p-value = 4.4x10-7), respectively. Additional file 1 presents all significant eQTLs based on the effective number of independent tests.

2.1.2. Expression trans and DE trans eQTL analysis, and master regulators

Twenty-seven SNPs (Table 1) distributed in 22 clusters (Figure 1) were identified and used to map potential master regulator genes. Figure 3 shows a network for the identified master regulators and their 674 associated genes (Additional file 2). Out of the 27 master regulators, nine membrane associated proteins, three cytoskeletal proteins, four transcription factors and one DNA methylase were identified. No clear classification was evident for the remaining ten genes. Figure 4 shows least-squares means plots for SNP effect on transformed gene counts for seven of the identified master regulators showing the effect on expression associated to hot spots such as rs378343630 and rs211476449.

2.1.3. Multigenic effects based on the eQTL analysis

Table 2 shows the distribution of eQTLs by gene in order to determine genes whose expression seems to be influenced by multiple genomic regions (Multigenic effects). The Solute Carrier Family 43 Member 1 (SLC43A1), Unc-51 Like Autophagy Activating Kinase 2 (ULK2), Myosin Light Chain 1 (MYL1), PHD Finger Protein 14 (PHF14), and Enolase 3 (ENO3) are the top five genes based on the number of eQTL regulators.

2.2. Splicing QTL mapping

The cis and trans sQTLs identified in the present analysis are presented in Figure 5 highlighting effects on DE genes. A total of 11,929 sQTLs were uncovered, where the trans sQTL being the most frequently identified type (Figure 2). Trans, DE trans, cis and DE cis effects were identified in 66.1, 16.9, 14.0 and 3.0% of the cases, respectively. The most frequently identified number of trans and DE trans sQTLs by SNP was one (88.4 and 88.9%, respectively).

2.2.1. Splicing cis and DE cis analysis

Additional file 1 shows all cis and DE cis sQTLs uncovered using the effective number of independent tests. Since the number of significant cis sQTLs detected using these threshold was very high, only associations with a p-value $\leq$ 2x10-4 were used for further analysis. A total of 2,222 cis sQTLs were identified and 16 were selected for further discussion (FDR $\leq$ 0.3). Two of the most interesting genes were Titin (TTN) and TEK Receptor Tyrosine Kinase (TEK).

2.2.2. Splicing trans and DE trans sQTL analysis, and master regulators

Out of the 13 splicing master regulator genes identified in the present analysis (Table 3), four encode for proteins located in the extracellular space, other four genes encode for plasma and/or organelle associated membrane proteins or cytoskeletal proteins, and other two encode for transcription factors. Mechanisms associated to splicing regulation for the remaining three master regulators were not evident. A total of 231 genes (Additional file 3) were associated with these 13 master regulators and included in a regulation network (Figure 6). The master regulators ZNF804A, ALAD, OR13F1 and ENSBTAG00000000336 were determined simultaneously as expression and splicing master regulators. Markers inside these four genes were able to explain variability in the fraction of exon counts in 28 (ZNF804A), 192 (ALAD), 22 (OR13F1) and 25 (ENSBTAG00000000336) genes across the genome. The most important uncovered master regulators associated with splicing were selected for further discussion.

Two different clusters were uncovered in the Functional Annotation Clustering analysis using the whole list of regulated genes across clusters (Additional file 4). Some of the identified terms in these clusters were Carbon metabolism, ATP binding and Nucleotide-binding, showing that genes in these clusters might have a complex splicing regulation and could be involved in differential biological functionality.

2.2.3. Multigenic effects based on the sQTL analysis

A variety of genes seem to have a complex transcriptional control based on the ratio of exon counts (Table 2) and some of them are: Titin (TTN), Nebulin (NEB), Elongin B (TCEB2), CAMP Responsive Element Binding Protein 5 (CREB5) and Upstream Transcription Factor 2, C-Fos Interacting (USF2).

Discussion

3.1. Expression QTL mapping

3.1.1. Expression cis and DE cis eQTL analysis

LSM2 binds to other members of the ubiquitous and multifunctional family Sm-like (LSM) in order to form RNA-processing complexes. These complexes are involved in processes such as stabilization of the spliceosomal U6 snRNA, mRNA decay and guide site-specific pseudouridylation of rRNA [5]. The hetero-heptameric complex LSM2-8 promotes small stable RNAs and pre-mRNAs nuclear processing meanwhile the LSM1-7 complex stimulates mRNA decapping and decay in the cytoplasm. The LSM2 subunit seems to be crucial for determining cellular location of this complex [6]. Lu et al. [7] identified two missense polymorphisms in SOAT1 associated with plasma cholesterol and triglyceride levels in mice. These SNPs increase enzyme activity despite similar gene expression levels. Although SOAT1 has been associated with cholesterol and triglyceride levels in mice, expression of this gene was not identified in the DE analysis in the present research.

3.1.2. Expression trans and DE trans eQTL analysis, and master regulators

The 27 master regulators identified in the eQTL analysis could contribute to gene expression control by promoting cell signaling or by direct transcriptional activation/repression mechanisms. The most important master regulators are described below.

Neurotrophin 3 (NTF3) was identified as master regulator in the present analysis since rs207649022 was able to explain variation in the expression of 76 genes (Table 1), 69.7% of which were DE genes (Figure 3B). The Neurotrophic Factor gene family regulates myoblast and muscle fiber differentiation. It also coordinates muscle innervation and functional differentiation of neuromuscular junctions [8]. Mice with only one functional copy of the NTF3 gene showed smaller cross-sectional fiber area and more densely distributed muscle fibers [9]. Upregulation of NTF3, stimulated by the transcription factor POU3F2, is present during neuronal differentiation [10]. The neocortex has multiple layers originated by cell fate restriction of cortical progenitors and NTF3 induces cell fate switches by controlling a feedback signal between postmitotic neurons and progenitors. Therefore, changes in NTF3 expression can modulate the amount of tissue present in each neocortex layer [11]. This gene was identified in a previous study as highly associated with cooking loss [12] pointing out that markers inside this locus are able to explain variation in both the phenotypic meat quality and the gene expression associated with meat quality. This provides positional and functional support for the potential role of NTF3 on meat quality. These effects seem not to be due to cis regulation on NTF3 giving that this gene was not expressed in skeletal muscle in the present population. However, NTF3 could be involved in earlier expression regulation based on its biological function. A Functional Annotation Clustering analysis for the NTF3 cluster indicated that the master regulator NTF3 could be involved in regulation of specific mechanisms and pathways related to Mitochondrion, Transit peptide and Mitochondrion inner membrane (Additional file 4).

The Phosphodiesterase 8B (PDE8B) was expressed in longissimus dorsi muscle in the present population. A SNP in this gene was found associated with expression levels of 27 genes, 74% of which were identified as DE genes related to meat quality. PDE8B hydrolyzes adenosine 3',5'-cyclic monophosphate (cAMP), and it is involved in a number of signal transduction pathways and physiological processes such as cell growth, cell differentiation, transcription and expression [13]. The cAMP-degrading enzymes have tight subcellular

localization, and control local cAMP and signal compartmentalization. Zhang et al. [14] reported that the phosphorylated cAMP-response Element Binding Protein (CREB) binds to approximately 4,000 promoter sites in vivo, depending on the methylation level of cAMP response elements near the promoter which highlights the role CREB plays in regulation of expression for a multitude of genes. CREB has a crucial role in neuronal membrane-to-nucleus signal transduction, regulate bone and cartilage remodeling by regulating the Matrix Metalloproteinase 1 (MMP1) and 13 (MMP13), stimulates promoter activity of adiponectin gene in adipocytes and inhibits the Cholesterol 7 α-Hydroxylase (CYP7A1) gene, which is involved in lipid homeostasis and bile acid synthesis in hepatocytes [15–17].

Expression of 36 genes was associated with rs211476449, a marker located in the Glutamate Decarboxylase 1 (GAD1) master regulator. This gene encodes a plasma membrane associated protein and downregulation of GAD1 has a detrimental effect on the cortical c-aminobutyric acid (GABA) system. This system has a paramount function on cellular proliferation and differentiation in multiple tissues [18].

FAT Atypical Cadherin 4 (FAT4) encodes a calcium-dependent cell adhesion transmembrane protein and it is involved in the Hippo signaling pathway. This pathway regulates organ size and tissue organization in vertebrates; when this gene is disrupted it alters oriented cell divisions. Inactivation of FAT4 promotes tumorigenesis in mammary epithelial cells and tumor progression is suppressed by FAT4 re-expression [19,20]. FAT is also involved in mammalian neurogenesis since downregulation of FAT in embryonic neuroepithelium in mice reduces the proportion of differentiated neurons [21]. Expression of 34 genes was associated with BTB_00676236, a marker located close to the master regulator FAT4.

The expression of 26 genes was associated with rs208227436, a polymorphism located in the master regulator Zinc Finger Protein 804A (ZNF804A). One polymorphism in the nuclear transmembrane protein ZNF804A gene is associated with schizophrenia and bipolar disorder; however, no function was identified for this gene. Since this protein has a zinc-finger domain, it was suggested that ZNF804A is involved in DNA binding and transcription regulation [22]. A direct interaction was reported between ZNF804A and the chromatin proximal to the promoter regions of several genes, some of them associated with cell adhesion and the Transforming Growth Factor-β (TGF-β) signaling pathway, probably influencing cell growth and differentiation.

The ENSBTAG00000035487 gene encodes a homologous of the Olfactory Receptor 4A47 (OR4A47) and the SNP rs109630111, was associated with expression of 36 genes. During perception of smell, olfactory receptors trigger signal transduction pathways by recognizing odorant molecules and these pathways might regulate apoptotic cycle of olfactory sensory neurons. Because these genes are expressed in non-olfactory related tissues, it is suggested that OR4A47 could have different biological functions [23]. Neuhaus et al. [24] and Ranzani et al [23] found expression of the olfactory receptor OR2C3 in human melanomas and documented that activation of OR51E2, another member of the olfactory receptor family, increases intracellular Ca2+, triggers some Mitogen-Activated Protein Kinases (MAPK) and inhibits cell proliferation.

Another master regulator, Paired Box 8 (PAX8) encodes a transcription factor involved in thyroid cell differentiation, and kidney and gonadal development. During kidney and kidney related tumor development, both transcription factors WT1 and PAX8 are co-expressed and since WT1 promoter has one PAX-binding site with enhancer activity, PAX8 is suggested as able to drive WT1 expression [25]. The plasma membrane associated protein Pleckstrin and Sec7 Domain Containing 4 (PSD4) activates ARF6, regulating its interaction with specific

plasma membrane subdomains and controlling reorganization of the actin cytoskeletal structure [26]. A total of 37 genes belong to the PAX8 cluster by being associated with rs209448226.

The SNP rs208451702 is located in RUNX1 Translocation Partner 1 (RUNX1T1 or Myeloid Translocation Gene on 8q22-MTG8) and explains expression variability in 24 other loci. It has transcriptional corepressor activity by recruiting other corepressors, and by interacting with DNA-binding transcription factors and histone-modifying enzymes. MTGs were recognized in acute myelogenous leukemia and mutations in this gene are associated with colon, breast and lung carcinoma, and have negative effects on the WNT and Notch signaling [27].

The rs377935001 marker is located in Tricopeptide Repeat Domain 25 (TTC25) gene and it was associated with expression of 34 genes. Deficient TTC25 mice lack the cilium outer dynein arms and its docking complex. The cilium is involved in motility and sensory-related processes such as left-right axis patterning, having a crucial developmental and homeostatic role [28,29].

The cytoskeleton associated protein Keratin 7 (KRT7) cluster shares some trans regulated genes with CSAD and was associated with expression of other 25 genes. The KRT7 is part of a keratin superfamily; KRT7 knockout mice have upregulated proliferation in bladder urothelium, KRT18 downregulation in bladder and KRT20 upregulation in superficial urothelial cells [30].

Lysine Demethylase 4A (KDM4A) cluster has 32 regulated genes associated with rs135786834; KDM4A encodes a histone lysine demethylase able to modify trimethylated H3-K9/K36 to dimethylated products, contributing to gene expression, cellular differentiation and cancer development [31]. Histone H3K9 methylation is used for silencing muscle specific genes in proliferating myoblasts and their derepression is required to initiate muscle differentiation; expression of a KDM4A isoform named DN-JMJD2A is upregulated during differentiation of myoblasts into myotubes promoting myotube formation and transcriptionally activating muscle-specific genes such as MyoD [32]. Hu et al. [33] reported that IOX1, an KDM4A inhibitor, is able to stall proliferation, migration and cell cycle progression by modulating cyclin D1 and p21 expression in angiotensin II stimulated vascular smooth muscle cells. This stalling process is mediated by promoter methylation. The only DE master regulator identified in the present analysis was KDM4A and this master regulator harbors rs135786834, a SNP associated with expression of 32 genes by trans association. Therefore, changes in expression of the master regulator KDM4A did not show evidence of promoting expression associated with meat quality inside its cluster.

Expression of 62 genes was associated with rs378343630, a marker located in the Transmembrane 4 L Six Family Member 1 (TM4SF1) master regulator. This gene encodes a plasma transmembrane protein and belongs to a gene family involved in signal transduction processes; thus, it modulates development, growth and motility [34]. The TM4SF1 protein physically interacts with membrane and some cytoskeleton-associated proteins to form cell projections named ‘nanopodia’ [35], which are described as frequently identified in multiple types of cancer. This gene is highly expressed in pancreatic cancer cells and stimulates metastasis by upregulating the Discoidin Domain Receptor Tyrosine Kinase 1 (DDR1) gene, Matrix Metallopeptidase 2 (MMP2) and Matrix Metallopeptidase 9 (MMP9) [36]. In liver, TM4SF1 reduced apoptosis and promoted cell migration by upregulating MMP-2, MMP-9 and VEGF, and downregulating Caspase-3 and Caspase-9 [34]. Upregulation of miR-9 produces downregulation of TM4SF1, MMP2, MMP9 and VEGF in colorectal carcinoma inhibiting cell migration and invasion [37]. In esophageal cancer stem-like cells, downregulation of miR-141 increases TM4SF1 expression, self-renewal ability and carcinogenicity, and promotes cell invasion and migration [38]. The

Functional Annotation Clustering analysis for TM4SF1 found overrepresentation of the transcription, DNA-templated term (Additional file 4); thus, TM4SF1 could be involved in regulation of specific mechanisms and pathways associated with transcription in longissimus dorsi muscle.

The master regulator GPR98 was identified as associated with tenderness from the sensory panel in the present population by Leal-Gutiérrez et al. (2019) and rs110618957, a polymorphism harbored by this gene, is able to explain variability in expression of 34 genes. GPR98 encodes a receptor associated with some bone related features in human and mice [39].

Pierce et al. [2] theorized that a high proportion of trans associations were caused by cis effects. However, no cis QTL was identified in any expression or splicing master regulator. The previous result seems to reveal that in the present analysis trans effects might contribute more to phenotypic variation related to meat quality than cis effects.

3.1.3. Multigenic effects based on the eQTL analysis

A total of 126 markers were identified as able to explain variation in SLC43A1 gene expression. This gene encodes a Na+-independent neutral amino acid transporter and it is upregulated in prostate cancer and hepatocarcinoma cells [40,41]. Forty three SNPs were associated with ULK2 expression. ULK2 is a serine/threonine protein kinase required for autophagy under nutrient-deprived conditions [42] and downregulation of ULK2 activates mTOR c1 signaling, promoting cell proliferation rates [43]. The MYL1 gene encodes a fast-twitch regulatory light chain of myosin in skeletal muscle; downregulation of MYL1 alters myocyte morphology and muscle structure, and generates congenital myopathy in zebrafish [44]; expression of MYL1 exclusively starts in fast-twitch cells during fast fibre differentiation [45]. A total of 40 and 36 polymorphisms were associated with MYL1 and PHF14 expression, respectively. PHF14 is ubiquitously expressed and its protein has multiple PHD fingers, a domain present in chromatin-binding proteins which is able to recognize particular epigenetic marks on histone tails. Knockout for PHF14 generates neonatal lethality and severe structural changes in multiple organs especially lungs in mice, being PHF14 an epigenetic regulator required for normal development of multiple organs and associated with some types of cancer [46,47]. Thirty six SNPs were associated with ENO3 expression and upregulation of ENO3 was evident in metastatic liver and muscle tissue [48]. These genes might have a tight expression regulation since multiple genomic regions are able to explain their expression.

3.2. Splicing QTL mapping

3.2.1. Splicing cis and DE cis analysis

The TTN gene harbors a DE cis sQTL (p-value = 2.0x10-7) and encodes a central sarcomeric protein. Some TTN mutations are associated with skeletal-muscle diseases such as tibial muscular dystrophy [49]. Fernandez-Marmiesse et al. [50] identified a non-sense mutation in a TTN exon only present in a fetal skeletal isoform and associated with a neuromuscular disorder; histologically, this mutation promotes sarcomeric deposition of a filamentous material.

A DE cis sQTL (p-value = 5.1x10-7) was identified in the TEK gene. The tyrosine kinase TEK encodes a receptor for Angiopoietin-1 (ANGPT1), and this signaling pathway is critical for migration, sprouting and survival of

endothelial cells; TEK activates the SHC Adaptor Protein 1 (SHC1), a protein involved in triggering the Ras/mitogen-activated protein kinase pathway, regulating migration and endothelial organization induced by ANGPT1 [51]. An ANGPT1-TEK antagonist named Angiopoietin-2 (ANGPT2) is expressed in regions of vascular remodeling in mice and humans and its upregulation is able to stall blood vessel formation in mouse embryos [52].

3.2.2. Trans and DE trans splicing QTL analysis, and master regulators

The non-coding RNAs, Small Nucleolar RNA, H/ACA Box 3A (SNORA3) and Small Nucleolar RNA, H/ACA Box 19 (SNORA19) are small nucleolar RNA molecules (snoRNA); snoRNAs modulate stability, folding and interaction with proteins and more recently, functions such as mRNA editing, alternative splicing and posttranscriptional gene silencing were discovered [53]. However, no clear function about SNORA3 and SNORA19 was described. Exon expression of 34 exons from 17 genes and 20 exons from 15 genes were associated with the polymorphisms rs209617551 (SNORA3) and BTB_01634267 (SNORA19), respectively.

Expression of 33 exons from 21 genes was associated with the SNP rs381222773, located in Phosphodiesterase 9A (PDE9A). This gene encodes a metal ion-dependent enzyme. The subcellular location of PDE9A is the plasma membrane in almost all organs but in bladder, where it is a cytoplasmic protein. Several PDE9A isoforms are described in human and mouse brain, and their expression and subcellular compartmentalization are age and tissue dependent [54]. PDE9A regulates nuclear- and membrane-proximal cGMP, regulating cellular signaling, and being involved in multiple biological and metabolic processes. It is also associated with several human neurological disorders by modulating intraneuronal signal transmission [55]. Upregulation of PDE9A is noticed in hypertrophic cardiomyocytes and during heart failure, but this symptomology is attenuated by PDE9A downregulation [56].

Expression of 23 exons form 19 genes was associated with rs382101207, a SNP located in Ring Finger Protein 20 (RNF20). This protein stimulates global H2B ubiquitylation at lysine 120 and promotes activator-dependent transcription [57]. Upregulation of RNF20 stimulates H2B monoubiquitination and methylation at H3K4 and H3K79; it promotes expression of Homeobox genes, a group of transcription factors [58]. RNF20 regulates expression of H2A and H2B histones, p53, several protooncogenes, epidermal growth factor and promotes cell migration and tumorigenesis [59]. The RNF20/RNF20 (Bre1 complex) is documented as a tumor suppressor by upregulating a set of tumor suppressor genes and by contributing to genomic stability maintenance. Bre1 deficient cells presents a high frequency of DNA double-strand breaks (DSB), having abundant aberrant RNA-DNA structures (R-loops) as indicators of replication stress and genomic instability [58]. H2B ubiquitylation is required during embryonic stem cell differentiation, process induced by stimulation of RNF20 activity and stalling of the deubiquitinase USP44 [60].

3.2.3. Multigenic effects based on the sQTL analysis

The large number of sQTLs identified in genes like TTN (324) and NEB (63) could be related to gene size, since these genes were 275 and 219 kb long, respectively, which would increase the probability of being involved in trans regulation. On the other hand, some genes relatively small in size: TCEB2 (9.9 kb) and USF2 (3.9 kb) also had a large number of sQTLs (43 and 33, respectively) indicating a complex splicing regulation.

A total of 324 and 67 polymorphisms were associated with TTN and NEB ratio exon counts, respectively. TTN and NEB are involved in assembly and mechanical activity of striated muscles. Both proteins are large sarcomere filament-binding proteins uniformly expressed in skeletal muscle and multiple splicing events in the bovine homologous have been described; in human brain, NEB acts as an actin filament stabilizer, regulates neuronal length, it is involved in myofibrillogenesis, modulates thin filament length and allows proper muscle contraction [61]. NEB deficient mice present muscular weakness, they die 8-11 days after birth, and show altered regulation of calcium homeostasis and glycogen metabolism associated genes [61]. Mouse NEB has 166 exons and four alternative splicing regions, two of them in exons 127 and 128; in most muscles, young mice had higher expression of the isoform including the exon 127 while the isoform including the exon 128 was highly expressed in older mice, showing that there could exist isoform switching related to muscle maturation [62].

Thirty-three sQTLs were identified in CAMP Responsive Element Binding Protein 5 (CREB5); CREB5 is upregulated in several types of human cancer since it modulates cell cycle. Upregulation of CREB5 promotes liver, colorectal and epithelial ovarian cancer cell proliferation and is an indicative of poor prognosis.

A total of 33 sQTLs were identified for the Upstream Transcription Factor 2, C-Fos Interacting (USF2) gene. Cell cycle control and modulation of apoptosis are some of the cellular processes where USF2 is involved. Christensen et al. [63] and Jaiswal & Narayan [64] reported that miR-362-3p modulate expression of USF2, a transcription factor able to interact with E-boxes located in the promoter region of Adenomatous Polyposis Coli (APC); APC is able to promote cell cycle arrest and apoptosis, being its malfunctioning associated with colorectal carcinogenesis. DNA-binding assays for a polymorfism associated with thyroid cancer susceptibility located in the 5'UTR of FOXE1, showed that the alternative allele is able to recruit the transcription factor USF2 [65].

3.3. Gene expression and splicing regulation mechanisms by plasma and organelle associated proteins

Cell cytoskeleton provides cellular mechanical constraints and extracellular matrix stiffness [66]. However, structural proteins are involved in multiple biological processes different from the organizational ones, with signaling and cell fate being some of the most important ones. Cell signaling is crucial since it orchestrates cellular responses to different microenvironmental stimulus, and transcription repression-activation and splicing regulation are influenced by signaling proteins. A number of receptors, transmembrane linkers, cytoskeletal fibers and membrane associated transcription factors were previously associated with transcription repression-activation.

The OR4A47, GPR98, PDE9A, OR13F1 and SYT14 master regulators are also described as transmembrane proteins and this type of molecule is involved in cell signaling processes. Pandey et al. [67] reported that estrogen can signal using diverse receptors, the G Protein-Coupled Estrogen Receptor 1 (GPR30) being one of them. Stimulation of GPR30 by estrogen activates a transcription factor network that upregulates Cellular Communication Network Factor 2 (CCN2), promoting proliferation and cell migration. The master regulators GAD1 and TM4SF1 encode transmembrane linkers and the integrin family has some well described transmembrane proteins. Integrins can modulate signal transduction cascades involved in cell survival, proliferation, differentiation and organ development [68]. The dimer ITGA1-ITGB1 can stall Epidermal Growth Factor Receptor (EGFR) signaling by stimulating Protein Tyrosine Phosphatase, Non-Receptor Type 2 (PTPN2). The cytoplasmic domain of ITGA1 interacts with PTPN2 and decreases EGFR phosphorylation after Epidermal Growth Factor (EGF) stimulation [69].

The cytoskeletal proteins KRT7, FAT4, MYH14 and DNAH7 were identified as master regulators, showing that cytoskeletal proteins might drive transcription regulation promoting cellular mechanisms such as growth and apoptosis. Flouriot et al. [66] reported that actin network can regulate Myocardin Related Transcription Factor A (MRTFA) subcellular localization, a protein involved in growth-quiescence switch. High F/G actin ratio or mutant MRTFA cells showed higher global biosynthetic activity and open chromatin state, associated with extensive histone modifications. In Drosophila, Hippo tumor suppressor pathway controls organ size, and proteins such as Yorkie (human homologous Yes Associated Protein 1 -YAP), a transcriptional coactivator, and Hpo and Warts kinases (human homologous Serine/Threonine Kinase 3 -STK3- and Large Tumor Suppressor Kinase 1 -LATS1, respectively) belong to this pathway. YAP is negatively regulated by STK3 and LATS1. F-actin accumulation promotes overgrowth in Drosophila imaginal discs through modulating the activity of the Hippo pathway [70]. Zhao et al. [71] reported that cell detachment promoted by cytoskeleton reorganization induces phosphorylation and inactivation of YAP, a process required for anoikis, a type of anchorage-dependent apoptosis.

The expression master regulator ZNF804A can be classified as a membrane associated transcription factor. A better described member of this group is CAMP Responsive Element Binding Protein 3 Like 1 (CREB3L1). This gene encodes an endoplasmic reticulum transmembrane stress transducer with a basic leucine zipper (bZIP) transcription factor domain. As a response to endoplasmic reticulum stress in osteoblasts, CREB3L1 is subject of regulated intramembrane proteolysis and its cleaved bZIP domain translocates into the nucleus, where initiates gene transcription [72,73]. The promotor region of the Collagen Type I Alpha 1 Chain (COL1A1) has an unfolded protein response element (UPRE)-like sequence in its promoter region, allowing COL1A1 expression controlled by the membrane associated protein CREB3L1 [73].

Conclusions

The mapping analysis performed in this study provides a holistic insight into the regulatory network architecture in *longissimus dorsi* muscle in an Angus-Brahman population.

Multiple cis eQTLs and sQTLs effects were identified and *LSM2, SOAT1, TTN* and *TEK* are a few examples of regulatory genes. A total of 27 expression and 13 splicing master regulator genes were uncovered, mainly cytoskeletal or membrane associated proteins, transcription factors and DNA methylases. Cytoskeletal proteins provide mechanical constraints to the cell but they are also involved in processes such as signaling. Signaling is crucial since it coordinates cellular responses to different stimuli, and transcription repression-activation and splicing regulation are influenced by structural proteins. The *ZNF804A, ALAD, OR13F1* and *ENSBTAG00000000336* genes were identified as both expression and splicing master regulators.

We show that eQTL and sQTL mapping makes possible positional identification of potential expression and splicing master regulators. This approach identified master regulators associated with gene and isoform expression in skeletal muscle but was also focused on uncovering master regulators related to genes whose expression is able to explain variability in meat quality related phenotypes (DE genes) in cattle. The genes PDE8B, NTF3, ZNF445 and OR4S1 can be highlighted as master regulators associated with a high proportion of DE genes, being capable of contributing to phenotypic variability through modulating expression of key genes associated with meat quality.

Methods

5.1 Cattle population and phenotypic data

The University of Florida Institutional Animal Care and Use Committee number 201003744 approved the present research protocol. A total of 120 steers from the University of Florida Beef Unit multibreed Angus-Brahman herd born between 2013 and 2014 were used in this study (Elzo et al., 2016). This population can be classified into six different groups based on breed composition. In terms of Angus composition, the grouping was the following: 1 = 100 to 80%; 2 = 79 to 65%; 3 = 64 to 60% (Brangus); 4 = 59 to 40%; 5 = 39 to 20%; 6 = 19 to 0%. (Leal-Gutiérrez et al., 2018).

These animals were kept with their dams on bahiagrass pastures (*Paspalum notatum)* until weaning and received a complete mineral supplement (UF University Special Hi-Cu Mineral, University of Florida, Gainesville, Florida), and bermudagrass (Cynodon dactylon) hay and cotton-seed (Gossypium spp.) meal in the winter months (mid-December to mid-March). The calves were kept on bahiagrass pastures, and fed bahiagrass hay, concentrate (1.6–3.6 kg of soy hull pellets per day; 14.0% CP; 488 Pellet Medicated Weaning Ration, Lakeland Animal Nutrition, Lakeland, Florida) and a mineral supplement until yearling.

Yearling steers were transported to a contract feeder (2014: Suwannee Farms, O Brien, Florida; 2015: Quincey Farms, Chiefland, Florida), where they were provided a standard feedlot diet based on corn, protein, vitamins, and minerals until they reached a subcutaneous fat thickness over the ribeye of approximately 1.27 cm (Elzo et al., 2017). Cattle were transported to a commercial processing facility (FPL Food LLC., Augusta, Georgia) one day prior to harvest. Steers were harvested under USDA-FSIS inspection using captive bolt stun. The average slaughter weight was 573.34±54.79 kg at 12.91±8.69 months. After splitting the carcass, five to ten g of the *longissimus dorsi* muscle was collected, snapped-frozen in liquid nitrogen and stored at –80°C until RNA was extracted.

Phenotypes recorded on these steers included tenderness, connective tissue and juiciness determined by sensory panel, and marbling, cooking loss and WBSF according to the American Meat Science Association Sensory Guidelines [76]. Marbling was assessed on the ribeye muscle at the 12th/13th rib interface after ribbing the carcass and was recorded on a numerical scale by visual appraisal 48 hours *postmortem.* The grading was as follows: Practically Devoid = 100–199, Traces = 200–299, Slight = 300–399, Small = 400–499, Modest = 500–599, Moderate = 600–699, Slightly Abundant = 700–799, Moderately Abundant = 800–899, Abundant = 900–999.

From each animal, two 2.54 cm steaks from the 12th/13th rib interface of the *longissimus dorsi* muscle were collected, aged for 14 days at 4°C, and stored at −20°C at the Meat Science Laboratory of the University of Florida. Frozen steaks were allowed to thaw at 4°C for 24 hours and cooked to an internal temperature of 71°C on an open-hearth grill.

After cooking, the first steak was cooled at 4°C for 18 to 24 hours and six cores with a 1.27-cm diameter and parallel to the muscle fiber were sheared with a Warner-Bratzler head attached to an Instron Universal Testing Machine (model 3343; Instron Corporation, Canton, MA). The Warner-Bratzler head moved at a cross head speed of 200 mm/min. The average peak load (kg) of six cores from the same animal was analyzed. The weight lost during cooking was recorded and cooking loss was expressed as a percentage of the cooked weight out of the thaw weight. The second steak was cooked and assessed by the sensory panel. The sensory panel consisted of eight to eleven trained members, and six animals were assessed per session. Two 1x2.54 cm samples from each

steak were provided to each panelist. Sensory panel measurements analyzed by the sensory panelists included: tenderness (8 = extremely tender, 7 = very tender, 6 = moderately tender, 5 = slightly tender, 4 = slightly tough, 3 = moderately tough, 2 = very tough, 1 = extremely tough), juiciness (8 = extremely juicy, 7 = very juicy, 6 = moderately juicy, 5 = slightly juicy, 4 = slightly dry, 3 = moderately dry, 2 = very dry, 1 = extremely dry), and connective tissue (8 = none detected, 7 = practically none, 6 = traces amount, 5 = slight amount, 4 = moderate amount, 3 = slightly abundant, 2 = moderately abundant, 1 = abundant amount). For each phenotype, the average score by steak from all members of the panel was analyzed.

Marbling, WBSF, cooking loss, juiciness, tenderness and connective tissue were included in a principal component (PC) analysis using PROC FACTOR procedure of SAS [77], and a composited meat quality index for each animal was constructed using the first three PCs. The meat quality index was determined using the following formula:

[Due to technical limitations, this equation is only available as a download in the supplemental files section.]

Where PCS_{ij} is the PC score of the animal i for the PC_j and PCW_j is the weight of the PC_j (eigenvalue). The amount of variance explained by PC_1, PC_2 and PC_3 were 44.26%, 20.04% and 13.29%, respectively. The 120 animals were ranked using the meat quality index and 80 animals with extreme values were selected and used for RNA sequencing.

5.2 Genotyping and data quality control

Genomic DNA was extracted from blood using the DNeasy Blood & Tissue kit (Qiagen, Valencia, CA) and stored at −20°C. All animals were genotyped with the commercial GGP Bovine F−250 chip (GeneSeek, Inc., Lincoln, NE) which contains 221,077 single nucleotide polymorphisms (SNPs). After excluding markers with a minor allele frequency lower than 3% (at least 2 animals out of 80 for the less frequent genotype) and a calling rate < 0.9, a total of 112,042 SNPs were included in the association analysis. Quality control was implemented with JMP genomics 6.0 software [78]. The genotype data is available in the European Variation Archive website, accession number PRJEB24746.

5.3 RNA extraction, RNA-seq library preparation and sequencing

Nuclear RNA was extracted from muscle using TRIzol reagent (Thermo Fisher Scientific, Waltham, MA, USA) according to the manufacturer's protocol (Invitrogen, catalog no. 15596—026). RNA concentration was measured by NanoDrop 2000 spectrophotometer (Thermo Fisher Scientific, Waltham, MA, USA) and integrity was verified by formaldehyde gel. The mRNA samples were stored at −80°C. Isolation of the mRNA was performed using oligo-dT attached magnetic beads prior its reverse transcription and synthesis of double stranded cDNA. An RNA-seq library for each sample was constructed, multiplexed, and sequenced based on protocols of Illumina HiSeq 3000 PE100 platform (Illumina, San Diego, CA, USA) to generate 2×101 bp paired-end reads. RNA-seq data are available at the European Nucleotide Archive, accession number PRJEB31379.

5.4 Read quality control, paired-end read alignment and paired-end read counting

Read trimming was performed with PRINSEQ 0.20.4 software [79] using 3 bp sliding windows and 20 as phred threshold. Reads with more than 2 ambiguous bases were excluded from the analysis. Cutadapt version 1.8.1 software [80] was used to trim adapters, and reads shorter that 50 nts were excluded. FastQC 0.9.6 software

(https://www.bioinformatics.babraham.ac.uk/projects/fastqc/) was used to verify sequence quality of clean raw reads.

Tophat 2.1.0 [81] and Bowtie2 2.3.4 [82] were used to perform paired-end read mapping against the Btau_4.6.1 reference genome (http://emea.support.illumina.com/sequencing/sequencing_software/igenome.html#). HTSeq 0.9.1 software [83] was used to estimate gene paired-end read counts for all annotated genes, including paired-end reads uniquely mapped to known chromosomes. Exon counts per gene were determined using the RNA-Sequencing differential expression analysis pipeline DEXSeq [84,85]. Genes and exons with less than 10 counts across all 80 samples were excluded from the analysis. Indexing and sorting of the alignment files was performed using Samtools 1.9 software [86].

5.5 Differentially expressed genes, exons and isoforms associated with meat quality

Differential expression (DE) analysis was performed to identify genes, exons and isoforms whose expression was associated with meat quality. The procedures described by Seo et al. [87], Love et al. [88] and Jia et al. [89] were used to identify DE. Genes and exons with less than 10 counts, and isoforms with less than 10 FPKM across samples were excluded from the analysis.

The R package edgeR [90–92] was used to obtain normalized gene counts by applying the trimmed mean of M-values (TMM) normalization method. The R packages sfsmisc and MASS [91,93,94] were used to apply Huber's M-estimator based robust regression including all 80 samples used for RNA sequencing. The meat quality index was used as response variable. Gene expression was treated as a covariate and year of birth of the animal as fixed effect. A PCA analysis was carried out with the "PCA for population structure" work-flow of JMP [78], and population structure was accounted for by including its first PC as covariate in the model. Genes whose association test had a p-value lower than 0.05 were included in the DE list. The same analysis was performed for exon expression, and genes with at least three associated exons were included in the DE list.

Out of the 80 samples used for RNA sequencing, 40 (20 high and 20 low performance based on WBSF, tenderness or marbling) were included in the DE analysis. The R package DESeq2 version 1.20.0 [88] was used to identify DE genes, including year of birth, breed group and a categorical classification of each animal based on phenotype as fixed effects in the analysis. The categorical classification was as follows: tender vs tough using WBSF or tenderness and high vs low using marbling. Genes with a Benjamini-Hochberg adjusted p-value lower than 0.05 were determined as DE for WBSF and lower than 0.1 as DE for tenderness and marbling. The DE isoform analysis was performed with MetaDiff [89]. Breed group, year of birth, and the same categorical classification based on phenotype fitted in the DESeq2 analysis were included as fixed effects in the association model.

A total of 8,799 genes, 93,349 exons, and 4,471 isoforms from 957 genes were included in the DE analysis. Expression of 1,352 genes was identified as associated with meat quality traits using the differential expression analysis (Additional file 5).

5.6 eQTL and sQTL mapping

The R package Matrix eQTL was used to perform the QTL mapping [91,95] using 112,042 SNPs and 8,588 genes (eQTL mapping) or 87,770 exons from 8,467 genes (sQTL mapping) located in autosomes. A linear regression

model was used where the SNP genotypes were coded as 0, 1 or 2. For the eQTL analysis, gene counts were transformed using the tool varianceStabilizingTransformation from the R package DESeq2 version 1.20.0 [88] in order to solve heteroscedasticity [96]. In the sQTL analysis we used the fraction of counts mapped to a specific exon out of the total counts mapped to its gene [97]. This fraction was converted to an integer value by keeping three decimal digits and multiplying by 1,000 and then transformed using the tool varianceStabilizingTransformation. Gene and fraction exon counts were included as response variables, and SNP genotype and year of birth of the animal as fixed effects. The first PC from the “PCA for population structure” work-flow of JMP [78] was included as a covariate in the model to control for population structure. A cis QTL was defined as a SNP located no more than 1 Mb upstream of the transcription start site or downstream of the transcription end site of an annotated gene, and cis and trans QTLs were analyzed separately.

Bonferroni trans and cis p-value thresholds were calculated using the effective number of independent tests implemented in the R function “simpleM_Ex” [98,99]. For the trans associations the total number of tests was 112,042, and 42,246 was its corresponding effective number of independent tests. Therefore, the p-value corrected for multiple testing for the trans effects was equal to $1.18x10^{-6}$ for both, trans eQTLs and sQTLs. However, in order to maximize the number of eQTLs and sQTLs hotspots a less stringent threshold was used. The final trans association thresholds used for eQTLs and sQTLs were $1x10^{-5}$ and $1x10^{-6}$, respectively. An effective number of independent tests per each gene was calculated in order to determine cis p-value thresholds. An in-house script written in Java was used to group all SNPs by gene and to generate the file inputs for the R function “simpleM_Ex” [98,99]. The Bonferroni cis p-value thresholds are presented in the Additional file 6. However, since the number of cis sQTLs was very high using this thresholds, a more stringent threshold was implemented. The final cis sQTL association threshold was $2x10^{-4}$.

Polymorphisms associated with expression of at least 20 genes in the case of eQTL and at least 20 exons in the case of sQTL were considered hot spot. The harboring gene or the adjacent gene which biological function was somewhat related to transcription regulation was defined as master regulators.

5.7 Functional annotation clustering analysis

A functional classification analysis using DAVID Bioinformatic Resources 6.8 server [100] was performed for each cluster of genes associated with a master regulator.

List Of Abbreviations

Quantitative trait loci (QTL)

Expression quantitative trait loci (eQTL)

Splicing quantitative trait loci (sQTL)

Differential expression (DE)

Single nucleotide polymorphism (SNP)

Declarations

7.1 Ethics approval and consent to participate

The research protocol was approved by the University of Florida Institutional Animal Care and Use Committee number 201003744.

7.2 Consent for publication

Not Applicable

7.3 Availability of data and material

Genotype data are available in the EVA website, accession number PRJEB24746. https://www.ebi.ac.uk/ena/data/view/PRJEB24746. RNA-seq data are available at the European Nucleotide Archive, accession number PRJEB31379, https://www.ebi.ac.uk/ena/data/search?query = PRJEB31379.

7.4 Competing interests

No commercial or financial relationships that could be construed as a potential conflict of interest exist.

7.5 Funding

Financial support provided by Florida Agricultural Experiment Station Hatch FLA-ANS–005548, Florida Beef Council, and Florida Beef Cattle Association—Beef Enhancement Fund Award 022962. The funders were not involved in the study design or collection, analysis, or interpretation of the data.

7.6 Authors' contributions

JL conducted all analyses and drafted the manuscript; ME assisted with the analysis and manuscript; RM conceived and assisted with the analyses and manuscript.

7.7 Acknowledgements

Not Applicable

References

1. Stranger BE, Nica AC, Forrest MS, Dimas A, Bird CP, Beazley C, et al. Population genomics of human gene expression. Nat Genet. 2007;39:1217–24.
2. Pierce BL, Tong L, Chen LS, Rahaman R, Argos M, Jasmine F, et al. Mediation Analysis Demonstrates That Trans-eQTLs Are Often Explained by Cis-Mediation: A Genome-Wide Analysis among 1,800 South Asians. PLoS Genet. 2014;10.
3. Liu H, Luo X, Niu L, Xiao Y, Chen L, Liu J, et al. Distant eQTLs and Non-coding Sequences Play Critical Roles in Regulating Gene Expression and Quantitative Trait Variation in Maize. Mol Plant. Elsevier Ltd; 2017;10:414–26.
4. Ponsuksili S, Murani E, Schwerin M, Schellander K, Wimmers K. Identification of expression QTL (eQTL) of genes expressed in porcine M. longissimus dorsi and associated with meat quality traits. BMC Genomics

[Internet]. BioMed Central Ltd; 2010;11:572. Available from: http://www.biomedcentral.com/1471–2164/11/572

5. Fernandez C, Pannone B, Chen X, Fuchs G, Wolin S. Rab11 in Recycling Endosomes Regulates the Sorting and Basolateral Transport of E-Cadherin. Mol Biol Cell [Internet]. 2004;15:2842–52. Available from: http://www.molbiolcell.org/cgi/doi/10.1091/mbc.E04?10?0867
6. Spiller MP, Reijns MAM, Beggs JD. Requirements for nuclear localization of the Lsm2–8p complex and competition between nuclear and cytoplasmic Lsm complexes. J Cell Sci. 2007;120:4310–20.
7. Lu Z, Yuan Z, Miyoshi T, Wang Q, Su Z, Chang CC. Identification of Soat1 as a Quantitative Trait Locus Gene on Mouse Chromosome 1 Contributing to Hyperlipidemia. PLoS One. 2011;6:1–8.
8. Chevrel G, Hohlfeld R, Sendtner M. The role of neurotrophins in muscle under physiological and pathological conditions. Muscle and Nerve. 2006;33:462–76.
9. Sheard PW, Bewick GS, Woolley AG, Shaw J, Fisher L, Fong SW, et al. Investigation of neuromuscular abnormalities in neurotrophin–3-deficient mice. Eur J Neurosci. 2010;31:29–41.
10. Lin YMJ, Hsin IL, Sun HS, Lin S, Lai YL, Chen HY, et al. NTF3 Is a Novel Target Gene of the Transcription Factor POU3F2 and Is Required for Neuronal Differentiation. Mol Neurobiol. Molecular Neurobiology; 2018;55:8403–13.
11. Parthasarathy S, Srivatsa S, Nityanandam A, Tarabykin V. Ntf3 acts downstream of Sip1 in cortical postmitotic neurons to control progenitor cell fate through feedback signaling. Development. 2014;141:3324–30.
12. Leal-Gutiérrez JD, Elzo MA, Johnson DD, Hamblen H, Mateescu RG. Genome wide association and gene enrichment analysis reveal membrane anchoring and structural proteins associated with meat quality in beef. BMC Genomics [Internet]. BMC Genomics; 2019;20:151. Available from: https://bmcgenomics.biomedcentral.com/articles/10.1186/s12864–019–5518–3
13. Yan K, Gao LN, Cui YL, Zhang Y, Zhou X. The cyclic AMP signaling pathway: Exploring targets for successful drug discovery (review). Mol Med Rep. 2016;13:3715–23.
14. Zhang X, Odom DT, Koo S-H, Conkright MD, Canettieri G, Best J, et al. Genome-wide analysis of cAMP-response element binding protein occupancy, phosphorylation, and target gene activation in human tissues. Proc Natl Acad Sci [Internet]. 2005;102:4459–64. Available from: http://www.pnas.org/cgi/doi/10.1073/pnas.0501076102
15. Benito E, Valor L, Jimenez-Minchan M, Huber W, Barco A. cAMP Response Element-Binding Protein Is a Primary Hub of Activity-Driven Neuronal Gene Expression. J Neurosci. 2011;31:18237–50.
16. Bui C, Barter M, Scott J, Xu Y, Galler M, Reynard L, et al. cAMP response element-binding (CREB) recruitment following a specific CpG demethylation leads to the elevated expression of the matrix metalloproteinase 13 in human articular chondrocytes and osteoarthritis. FASEB J. 2012;26:3000–11.
17. Song KH, Chiang JYL. Glucagon and cAMP inhibit cholesterol 7α-hydroxylase (CYP7A1) gene expression in human hepatocytes: Discordant regulation of bile acid synthesis and gluconeogenesis. Hepatology. 2006;43:117–25.
18. Addington AM, Gornick M, Duckworth J, Sporn A, Gogtay N, Bobb A, et al. GAD1 (2q31.1), which encodes glutamic acid decarboxylase (GAD 67), is associated with childhood-onset schizophrenia and cortical gray matter volume loss. Mol Psychiatry. 2005;10:581–8.

19. Chao Q, Yiwei TZ, Liping H, Zhu YJ. Identification of Fat4 as a candidate tumor suppressor gene In breast cancers. Int J Cancer. 2009;124:793–8.
20. Saburi S, Hester I, Fischer E, Pontoglio M, Eremina V, Gessler M, et al. Loss of Fat4 disrupts PCP signaling and oriented cell division and leads to cystic kidney disease. Nat Genet. 2008;40:1010–5.
21. Cappello S, Gray MJ, Badouel C, Lange S, Einsiedler M, Srour M, et al. Mutations in genes encoding the cadherin receptor-ligand pair DCHS1 and FAT4 disrupt cerebral cortical development. Nat Genet [Internet]. Nature Publishing Group; 2013;45:1300–10. Available from: http://dx.doi.org/10.1038/ng.2765
22. Girgenti MJ, LoTurco JJ, Maher BJ. ZNF804a regulates expression of the schizophrenia-associated genes PRSS16, COMT, PDE4B, and DRD2. PLoS One. 2012;7:2–6.
23. Ranzani M, Iyer V, Ibarra-Soria X, Del Castillo Velasco-Herrera M, Garnett M, Logan D, et al. Revisiting olfactory receptors as putative drivers of cancer. Wellcome Open Res [Internet]. 2017;2:9. Available from: https://wellcomeopenresearch.org/articles/2–9/v1
24. Neuhaus EM, Zhang W, Gelis L, Deng Y, Noldus J, Hatt H. Activation of an olfactory receptor inhibits proliferation of prostate cancer cells. J Biol Chem. 2009;284:16218–25.
25. Fraizer GC, Shimamura R, Zhang X, Saunders GF. PAX 8 regulates human WT1 transcription through a novel DNA binding site. J Biol Chem. 1997;272:30678–87.
26. Derrien V, Couillault C, Franco M, Martineau S, Montcourrier P, Houlgatte R, et al. A conserved C-terminal domain of EFA6-family ARF6- guanine nucleotide exchange factors induces lengthening of microvilli-like membrane protrusions. J Cell Sci. 2002;115:2867–79.
27. Wood AR, Esko T, Yang J, Vedantam S, Pers TH, Gustafsson S, et al. Defining the role of common variation in the genomic and biological architecture of adult human height. Nat Genet [Internet]. 2014;46:1173–86. Available from: http://www.nature.com/doifinder/10.1038/ng.3097
28. Sigg MA, Menchen T, Lee C, Johnson J, Jungnickel MK, Choksi SP, et al. Evolutionary Proteomics Uncovers Ancient Associations of Cilia with Signaling Pathways. Dev Cell [Internet]. Elsevier Inc.; 2017;43:744–762.e11. Available from: https://doi.org/10.1016/j.devcel.2017.11.014
29. Wallmeier J, Shiratori H, Dougherty GW, Edelbusch C, Hjeij R, Loges NT, et al. TTC25 Deficiency Results in Defects of the Outer Dynein Arm Docking Machinery and Primary Ciliary Dyskinesia with Left-Right Body Asymmetry Randomization. Am J Hum Genet [Internet]. American Society of Human Genetics; 2016;99:460–9. Available from: http://dx.doi.org/10.1016/j.ajhg.2016.06.014
30. Sandilands A, Smith FJD, Lunny DP, Campbell LE, Davidson KM, MacCallum SF, et al. Generation and Characterisation of Keratin 7 (K7) Knockout Mice. PLoS One. 2013;8:1–11.
31. Guerra-Calderas L, González-Barrios R, Herrera LA, de León DC, Soto-Reyes E. The role of the histone demethylase KDM4A in cancer. Cancer Genet. 2015;208:215–24.
32. Verrier L, Escaffit F, Chailleux C, Trouche D, Vandromme M. A new isoform of the histone demethylase JMJD2A/KDM4A is required for skeletal muscle differentiation. PLoS Genet. 2011;7.
33. Hu Q, Chen J, Zhang J, Xu C, Yang S, Jiang H. IOX1, a JMJD2A inhibitor, suppresses the proliferation and migration of vascular smooth muscle cells induced by angiotensin II by regulating the expression of cell cycle-related proteins. Int J Mol Med. 2016;37:189–96.
34. Huang YK, Fan XG, Qiu F. TM4SF1 promotes proliferation, invasion, and metastasis in human liver cancer cells. Int J Mol Sci. 2016;17:1–19.

35. Zukauskas A, Merley A, Li D, Ang LH, Sciuto TE, Salman S, et al. TM4SF1: A tetraspanin-like protein necessary for nanopodia formation and endothelial cell migration. Angiogenesis. 2011;14:345–54.
36. Yang JC, Zhang Y, He SJ, Li MM, Cai XL, Wang H, et al. TM4SF1 Promotes Metastasis of Pancreatic Cancer via Regulating the Expression of DDR1. Sci Rep [Internet]. Nature Publishing Group; 2017;7:3–10. Available from: http://dx.doi.org/10.1038/srep45895
37. Park Y, Lee S, Kim S, Liu Y, Lee M, Shin J, et al. MicroRNA–9 suppresses cell migration and invasion through downregulation of TM4SF1 in colorectal cancer. Int J Oncol. 2016;48:2135–413.
38. Xue L, Yu X, Jiang X, Deng X, Mao L, Guo L, et al. TM4SF1 promotes the self-renewal of esophageal cancer stem-like cells and is regulated by miR–141. Oncotarget. 2017;8:19274–84.
39. Urano T, Shiraki M, Yagi H, Ito M, Sasaki N, Sato M, et al. GPR98 / Gpr98 Gene Is Involved in the Regulation of Human and Mouse Bone Mineral Density. J Clin Endocrinol Metab [Internet]. 2012;97:E565–74. Available from: https://academic.oup.com/jcem/article-lookup/doi/10.1210/jc.2011–2393
40. Cole K, Chuaqui R, Katz K, Pack S, Zhuang Z, Cole C, et al. cDNA Sequencing and Analysis of POV1 (PB39): A Novel Gene Up-regulated in Prostate Cancer. Genomics. 2002;51:282–7.
41. Babu E, Kanai Y, Chairoungdua A, Kim DK, Iribe Y, Tangtrongsup S, et al. Identification of a Novel System L Amino Acid Transporter Structurally Distinct from Heterodimeric Amino Acid Transporters. J Biol Chem. 2003;278:43838–45.
42. Lee EJ, Tournier C. The requirement of uncoordinated 51-like kinase 1 (ULK1) and ULK2 in the regulation of autophagy. Autophagy. 2011;7:689–95.
43. Jung CH, Seo M, Otto NM, Kim DH. ULK1 inhibits the kinase activity of mTORC1 and cell proliferation. Autophagy. 2011;7:1212–21.
44. Ravenscroft G, Zaharieva I, Bortolotti CA, Lambrughi M, Pignataro M, Borsari M, et al. Bi-allelic mutations in MYL1 cause a severe congenital myopathy. Hum Mol Genet [Internet]. 2018;27:4263–72. Available from: https://academic.oup.com/hmg/advance-article/doi/10.1093/hmg/ddy320/5095322
45. Burguière AC, Nord H, Von Hofsten J. Alkali-like myosin light chain–1 (myl1) is an early marker for differentiating fast muscle cells in zebrafish. Dev Dyn. 2011;240:1856–63.
46. Huang Q, Zhang L, Wang Y, Zhang C, Zhou S, Yang G, et al. Depletion of PHF14, a novel histone-binding protein gene, causes neonatal lethality in mice due to respiratory failure. Acta Biochim Biophys Sin (Shanghai). 2013;45:622–33.
47. Akazawa T, Yasui K, Gen Y, Yamada N, Tomie A, Dohi O, et al. Aberrant expression of the PHF14 gene in biliary tract cancer cells. Oncol Lett. 2013;5:1849–53.
48. Chaika N, Yu F, Purohit V, Mehla K, Lazenby A, DiMaio D, et al. Differential expression of metabolic genes in tumor and stromal components of primary and metastatic loci in pancreatic adenocarcinoma. PLoS One. 2012;7:1–10.
49. Hackman P, Vihola A, Haravuori H, Marchand S, Sarparanta J, de Seze J, et al. Tibial Muscular Dystrophy Is a Titinopathy Caused by Mutations in TTN, the Gene Encoding the Giant Skeletal-Muscle Protein Titin. Am J Hum Genet [Internet]. 2002;71:492–500. Available from: http://www.ncbi.nlm.nih.gov/pubmed/12145747%5Cnhttp://www.pubmedcentral.nih.gov/articlerender.fcgi?artid = PMC379188%5Cnhttp://linkinghub.elsevier.com/retrieve/pii/S0002929707603309

50. Fernández-Marmiesse A, Carrascosa-Romero MC, Alfaro Ponce B, Nascimento A, Ortez C, Romero N, et al. Homozygous truncating mutation in prenatally expressed skeletal isoform of TTN gene results in arthrogryposis multiplex congenita and myopathy without cardiac involvement. Neuromuscul Disord [Internet]. Elsevier B. V.; 2017;27:188–92. Available from: http://dx.doi.org/10.1016/j.nmd.2016.11.002
51. Audero E, Cascone I, Maniero F, Napione L, Arese M, Lanfrancone L, et al. Adaptor ShcA Protein Binds Tyrosine Kinase Tie2 Receptor and Regulates Migration and Sprouting but Not Survival of Endothelial Cells. J Biol Chem. 2004;279:13224–33.
52. Maisonpierre P, Suri C, Jones P, Bartunkova S, Wiegand S, Radziejewski C, et al. Angiopoietin–2, a natural antagonist for Tie2 that disrupts in vivo angiogenesis. Science (80-) [Internet]. 1997;277:55–60. Available from: http://www.ncbi.nlm.nih.gov/entrez/query.fcgi?cmd = Retrieve&db = PubMed&dopt = Citation&list_uids = 9204896
53. Bratkovič T, Rogelj B. The many faces of small nucleolar RNAs. Biochim Biophys Acta - Gene Regul Mech. 2014;1839:438–43.
54. Patel NS, Klett J, Pilarzyk K, Lee D ik, Kass D, Menniti FS, et al. Identification of new PDE9A isoforms and how their expression and subcellular compartmentalization in the brain change across the life span. Neurobiol Aging [Internet]. Elsevier Inc; 2018;65:217–34. Available from: https://doi.org/10.1016/j.neurobiolaging.2018.01.019
55. Liu S, Mansour MN, Dillman KS, Perez JR, Danley DE, Aeed PA, et al. Structural basis for the catalytic mechanism of human phosphodiesterase 9. Proc Natl Acad Sci. 2008;105:13309–14.
56. Wang PX, Li ZM, Cai SD, Li JY, He P, Huang Y, et al. C33(S), a novel PDE9A inhibitor, protects against rat cardiac hypertrophy through upregulating cGMP signaling. Acta Pharmacol Sin [Internet]. Nature Publishing Group; 2017;38:1257–68. Available from: http://dx.doi.org/10.1038/aps.2017.38
57. Kim J, Hake SB, Roeder RG. The human homolog of yeast BRE1 functions as a transcriptional coactivator through direct activator interactions. Mol Cell. 2005;20:759–70.
58. Chernikova SB, Razorenova O V., Higgins JP, Sishc BJ, Nicolau M, Dorth JA, et al. Deficiency in mammalian histone H2B ubiquitin ligase Bre1 (Rnf20/Rnf40) leads to replication stress and chromosomal instability. Cancer Res. 2012;72:2111–9.
59. Shema E, Tirosh I, Aylon Y, Huang J, Ye C, Moskovits N, et al. The histone H2B-specific ubiquitin ligase RNF20/hBREl acts as a putative tumor suppressor through selective regulation of gene expression. Genes Dev. 2008;22:2664–76.
60. Fuchs G, Shema E, Vesterman R, Kotler E, Wolchinsky Z, Wilder S, et al. RNF20 and USP44 Regulate Stem Cell Differentiation by Modulating H2B Monoubiquitylation. Mol Cell [Internet]. Elsevier Inc.; 2012;46:662–73. Available from: http://dx.doi.org/10.1016/j.molcel.2012.05.023
61. Bang ML, Li X, Littlefield R, Bremner S, Thor A, Knowlton KU, et al. Nebulin-deficient mice exhibit shorter thin filament lengths and reduced contractile function in skeletal muscle. J Cell Biol. 2006;173:905–16.
62. Donner K, Nowak KJ, Aro M, Pelin K, Wallgren-Pettersson C. Developmental and muscle-type-specific expression of mouse nebulin exons 127 and 128. Genomics. 2006;88:489–95.
63. Christensen L, Tobiasen H, Holm A, Schepeler T, Ostenfeld M, Thorsen K, et al. MiRNA–362–3p induces cell cycle arrest through targeting of E2F1, USF2 and PTPN1 and is associated with recurrence of colorectal cancer. Int J Cancer. 2013;133:67–78.

64. Jaiswal AS, Narayan S. Upstream stimulating factor–1 (USF1) and USF2 bind to and activate the promoter of the adenomatous polyposis coil (APC) tumor suppressor gene. J Cell Biochem. 2001;81:262–77.
65. Landa I, Ruiz-Llorente S, Montero-Conde C, Inglada-Pérez L, Schiavi F, Leskelä S, et al. The variant rs1867277 in FOXE1 gene confers thyroid cancer susceptibility through the recruitment of USF1/USF2 transcription factors. PLoS Genet. 2009;5:5–10.
66. Flouriot G, Huet G, Boujrad N, Demay F, Pakdel F, Michel D. The actin/MKL1 signalling pathway influences cell growth and gene expression through large-scale chromatin reorganization and histone post-translational modifications. Biochem J. 2014;461:257–68.
67. Pandey DP, Lappano R, Albanito L, Madeo A, Maggiolini M, Picard D. Estrogenic GPR30 signalling induces proliferation and migration of breast cancer cells through CTGF. EMBO J. 2009;28:523–32.
68. Zhang Y, Wang H. Integrin signalling and function in immune cells. Immunology. 2012;135:268–75.
69. Mattila E, Pellinen T, Nevo J, Vuoriluoto K, Arjonen A, Ivaska J. Negative regulation of EGFR signalling through integrin-α1β1-mediated activation of protein tyrosine phosphatase TCPTP. Nat Cell Biol. 2004;7:78–85.
70. Sansores-Garcia L, Bossuyt W, Wada KI, Yonemura S, Tao C, Sasaki H, et al. Modulating F-actin organization induces organ growth by affecting the Hippo pathway. EMBO J [Internet]. Nature Publishing Group; 2011;30:2325–35. Available from: http://dx.doi.org/10.1038/emboj.2011.157
71. Zhao B, Li L, Wang L, Wang CY, Yu J, Guan KL. Cell detachment activates the Hippo pathway via cytoskeleton reorganization to induce anoikis. Genes Dev. 2012;26:54–68.
72. Kondo S, Murakami T, Tatsumi K, Ogata M, Kanemoto S, Otori K, et al. OASIS, a CREB/ATF-family member, modulates UPR signalling in astrocytes. Nat Cell Biol. 2005;7:186–94.
73. Murakami T, Saito A, Hino SI, Kondo S, Kanemoto S, Chihara K, et al. Signalling mediated by the endoplasmic reticulum stress transducer OASIS is involved in bone formation. Nat Cell Biol [Internet]. Nature Publishing Group; 2009;11:1205–11. Available from: http://dx.doi.org/10.1038/ncb1963
74. Elzo MA, Mateescu R, Thomas MG, Johnson DD, Martinez CA, Rae DO, et al. Growth and reproduction genomic-polygenic and polygenic parameters and prediction trends as Brahman fraction increases in an Angus-Brahman multibreed population. Livest Sci [Internet]. Elsevier; 2016;190:104–12. Available from: http://dx.doi.org/10.1016/j.livsci.2016.06.011
75. Leal-Gutiérrez JD, Elzo MA, Johnson DD, Scheffler TL, Scheffler JM, Mateescu RG. Association of μ-Calpain and Calpastatin Polymorphisms with Meat Tenderness in a Brahman–Angus Population. Front Genet [Internet]. 2018;9:1–10. Available from: http://journal.frontiersin.org/article/10.3389/fgene.2018.00056/full
76. Belk KE, Dikeman ME, Calkins CR, Andy King D, Shackelford SD, Hale D, et al. Research Guidelines for Cookery, Sensory Evaluation, and Instrumental Tenderness Measurements of Meat. 2015.
77. SAS Institute, Inc., Cary, NC. United States;
78. JMP®, Version 13. SAS Institute Inc., Cary, NC, 1989–2007.
79. Schmieder R, Edwards R. Quality control and preprocessing of metagenomic datasets. Bioinformatics. 2011;27:863–4.
80. Martin M. Cutadapt removes adapter sequences from high-throughput sequencing reads. EMBnet.journal [Internet]. 2011;17:10. Available from: http://journal.embnet.org/index.php/embnetjournal/article/view/200

81. Kim D, Pertea G, Trapnell C, Pimentel H, Kelley R, Salzberg S. TopHat2: accurate alignment of transcriptomes in the presence of insertions, deletions and gene fusions. Genome Biol. 2013;14:0–9.
82. Langmead B, Salzberg SL. Fast gapped-read alignment with Bowtie 2. Nat Methods. 2012;9:357–9.
83. Anders S, Pyl P, Huber W. HTSeq-A Python framework to work with high-throughput sequencing data. Bioinformatics. 2015;31:166–9.
84. Anders S, Reyes A, Huber W. Detecting diferential usage of exons from RNA-seq data. Genome Res [Internet]. 2012;22:2008–17. Available from: http://dx.doi.org/10.1101/gr.133744.111
85. Reyes A, Anders S, Weatheritt RJ, Gibson TJ, Steinmetz LM, Huber W. Drift and conservation of differential exon usage across tissues in primate species. Proc Natl Acad Sci [Internet]. 2013;110:15377–82. Available from: http://www.pnas.org/cgi/doi/10.1073/pnas.1307202110
86. Li H, Handsaker B, Wysoker A, Fennell T, Ruan J, Homer N, et al. The Sequence Alignment/Map format and SAMtools. Bioinformatics. 2009;25:2078–9.
87. Seo M, Kim K, Yoon J, Jeong JY, Lee HJ, Cho S, et al. RNA-seq analysis for detecting quantitative trait-associated genes. Sci Rep [Internet]. Nature Publishing Group; 2016;6:1–12. Available from: http://dx.doi.org/10.1038/srep24375
88. Love MI, Huber W, Anders S. Moderated estimation of fold change and dispersion for RNA-seq data with DESeq2. Genome Biol. 2014;15:1–21.
89. Jia C, Guan W, Yang A, Xiao R, Tang WHW, Moravec CS, et al. MetaDiff: Differential isoform expression analysis using random-effects meta-regression. BMC Bioinformatics. BMC Bioinformatics; 2015;16:1–12.
90. McCarthy DJ, Chen Y, Smyth GK. Differential expression analysis of multifactor RNA-Seq experiments with respect to biological variation. Nucleic Acids Res. 2012;40:4288–97.
91. R Core Team. R: A language and environment for statistical computing. R Foundation for Statistical Computing [Internet]. Vienna, Austria; 2018. Available from: http://www.r-project.org.
92. Robinson MD, McCarthy DJ, Smyth GK. edgeR: A Bioconductor package for differential expression analysis of digital gene expression data. Bioinformatics. 2010;26:139–40.
93. Maechler M. sfsmisc: Utilities from “Seminar fuer Statistik” ETH Zurich. R package version 1.1–2. [Internet]. 2018. Available from: https://cran.r-project.org/package = sfsmisc
94. Venables WN, Ripley BD. Modern Applied Statistics with S. Fourth Edi. Springer, New York; 2002.
95. Shabalin AA. Matrix eQTL: Ultra fast eQTL analysis via large matrix operations. Bioinformatics. 2012;28:1353–8.
96. Higgins MG, Fitzsimons C, McClure MC, McKenna C, Conroy S, Kenny DA, et al. GWAS and eQTL analysis identifies a SNP associated with both residual feed intake and GFRA2 expression in beef cattle. Sci Rep. 2018;8:1–12.
97. Pickrell J, Marioni J, Pai A, Degner J, Engelhardt B, Nkadori E, et al. Understanding mechanisms underlying human gene expression variation with RNA sequencing. Nature [Internet]. Nature Publishing Group; 2010;464:768–72. Available from: http://dx.doi.org/10.1038/nature08872
98. Gao X, Starmer J, Martin ER. A multiple testing correction method for genetic association studies using correlated single nucleotide polymorphisms. Genet Epidemiol. 2008;32:361–9.
99. Gao X, Becker LC, Becker DM, Starmer JD, Province M. Avoiding the high Bonferroni penalty in genome-wide association studies. Genet Epidemiol. 2010;34:100–5.

100. Huang DW, Sherman BT, Lempicki RA. Systematic and integrative analysis of large gene lists using DAVID bioinformatics resources. Nat Protoc. 2009;4:44–57.

Tables

Table 1. Expression QTL master regulators identified in *longissimus dorsi* muscle sampled from a multibreed Angus-Brahman herd. SNP information on 112,042 markers, and expression data from 8,588 genes were included in the association assay. Out of the 8,588 genes included, 1,352 genes were previously identified as differentially expressed (DE genes) in the present population..

SNP location	SNP name	Cluster*	MAF (%)	Number of eQTLs	% DE eQTLs	Harboring gene or closest genes +
1: 119,758,395	rs378343630	1	4	62	0.0	*TM4SF1*
2: 11,594,176	rs208227436	2	3	26	7.7	*ZNF804A*
2: 25,653,736	rs211476449	3	3	36	13.9	*GAD1*
3: 102,943,677	rs135786834	4	2	32	0.0	*KDM4A*
5: 27,001,953	rs441241989	5	8	27	18.5	*CSAD*
5: 27,834,250	rs110130901	5	8	25	24.0	*KRT7*
5: 105,380,442	rs207649022	6	24	76	69.7	***NTF3*** *- KCNA5*
7: 92,439,344	rs110618957	7	2	34	8.8	*POLR3G -* ***GPR98***
8: 95,625,807	ARS_BFGL_N-GS_65636	8	3	111	8.1	*ENSBTAG00000047350 -* ***OR13F1***
8: 104,345,143	rs378706947	8	2	22	9.1	*ALAD*
10: 8,457,276	Bovine-HD1000002801	9	30	27	74.1	*PDE8B*
11: 46,753,639	rs211218494	10	8	37	13.5	*PSD4*
11: 46,785,388	rs209448226	10	8	37	13.5	*5S_rRNA -* ***PAX8***
13: 54,009,694	rs135144232	11	4	24	8.3	*ENSBTAG00000011638*
14: 74,732,269	rs208451702	12	3	24	8.3	*RUNX1T1*
15: 79,202,054	rs41781450	13	37	20	35.0	*OR4X1 -* ***OR4S1***
15: 79,564,333	rs109630111	13	24	36	2.8	*ENSBTAG00000035487*
16: 62,544,863	rs456174577	14	2	36	0.0	*TOR1AIP1*
17: 30,508,078	BTB_00676236	15	41	34	23.5	*INTU -* ***FAT4***
18: 56,858,212	rs41891374	16	5	20	20.0	*C18H19ORF41 -* ***MYH14***
18: 57,361,426	rs383445569	16	4	41	17.1	*KLK4*
18: 61,257,126	No SNP name	17	49	133	2.3	***ENSBTAG00000000336*** *- ENSBTAG00000046961*
19: 42,754,262	rs377935001	18	2	34	0.0	*TTC25*
22: 16,367,834	rs110289782	19	11	24	50.0	*ENSBTAG00000030533 -* ***ZNF445***
26: 12,930,282	rs42085062	20	4	23	26.1	*PCGF5*
27: 31,921,721	rs136162903	21	3	25	0.0	*KCNU1*
28:	rs207999887	22	5	34	5.9	*SNORA25 -* ***SIPA1L2***

4,877,558

* Cluster number used in Figure 1.

+ Bolded genes were selected as master regulators when the associated SNP was intergenic; underlined gene names were identified as expressed in skeletal muscle in the present analysis.

Table 2. Number and effect type for multigenic effects from the eQTL and sQTL analysis performed in *longissimus dorsi* muscle sampled from a multibreed Angus-Brahman herd. SNP information on 112,042 markers, and expression data from 8,588 genes and 87,770 exons from 8,467 genes were included in the association analysis.

eQTL analysis			sQTL analysis		
SLC43A1	126	Trans	*TTN*	324	DE Trans
LOC100848703	64	Trans	*TXN2*	99	Trans
ULK2	43	Trans	*NEB*	63	DE Trans
MYL1	40	Trans	*TCEB2*	43	Trans
ENO3	36	Trans	*LOC100851645*	36	DE Trans
PHF14	36	Trans	*CREB5*	33	DE Trans
PKM	32	Trans	*USF2*	33	DE Trans
ZBTB12	31	Trans	*MYH7*	28	Trans
PGAM2	30	Trans	*PON3*	26	Trans
ACTA1	28	Trans	*MYOM3*	26	Trans
SNX19	25	Trans	*RSPO2*	25	Trans
LDHA	25	Trans	*METTL22*	25	Trans
RPL5	23	Trans	*MAP3K14*	25	Trans
ALDH4A1	23	DE Trans	*UBR3*	25	Trans
PLSCR3	22	Trans	*PAPD4*	25	Trans
CHURC1	22	Trans	*BAZ1A*	24	Trans
TNNI2	22	Trans	*ITPR1*	23	Trans
GPD1	21	Trans	*MYH1*	23	Trans
TMTC2	21	Trans	*SVIL*	22	Trans
UCK2	21	DE Trans	*ZDHHC4*	22	Trans
LRRC42	20	Trans	*FILIP1L*	22	DE Trans
			HSPG2	21	Trans
			UBR4	21	Trans
			KTN1-2	21	Trans
			DST	21	DE Trans
			MYBPC1	20	Trans

Table 3. sQTL master regulators identified in *longissimus dorsi* muscle sampled from a multibreed Angus-Brahman herd. SNP information on 112,042 markers, and expression data from 87,770 exons from 8,467 genes were included in the association analysis.

SNP location	SNP name	Cluster*	MAF (%)	Number of sQTLs	% DE eQTLs	Harboring gene or closest genes +
1: 144,604,558	rs381222773	1	7	33	90.9	***PDE9A*** - *WDR4*
2: 11,594,176	rs208227436	2	3	28	82.1	*ZNF804A*
2: 84,792,003	rs208053623	3	4	21	81.0	*DNAH7*
4: 5,827,343	rs381476620	4	42	21	66.7	*ZPBP* - ***VWC2***
8: 92,924,658	rs382101207	5	3	23	87.0	*RNF20*
8: 93,336,078	BTB_01634267	5	4	20	80.0	*PLEKHB2* - ***SNORA19***
8: 95,762,113	rs136343964	5	3	22	86.4	*OR13F1*
8: 104,345,143	rs378706947	6	2	192	72.9	*ALAD*
14: 57,184,022	rs210798753	7	2	24	50.0	*PKHD1L1*
15: 25,536,733	rs209617551	8	2	34	64.7	*SNORA3*
15: 35,729,304	rs382501844	9	4	33	90.9	*NUCB2* - *ENSBTAG00000032859*
16: 75,296,157	rs41821837	10	4	20	80.0	***SYT14*** - *DIEXF*
18: 61,257,126		11	49	25	56.0	***ENSBTAG00000000336*** - *ENSBTAG00000046961*

***** Cluster number used in Figure 5.

+ Bolded genes were selected as master regulators when the associated SNP was intergenic; underlined gene names were identified as expressed in skeletal muscle in the present analysis.

Figures

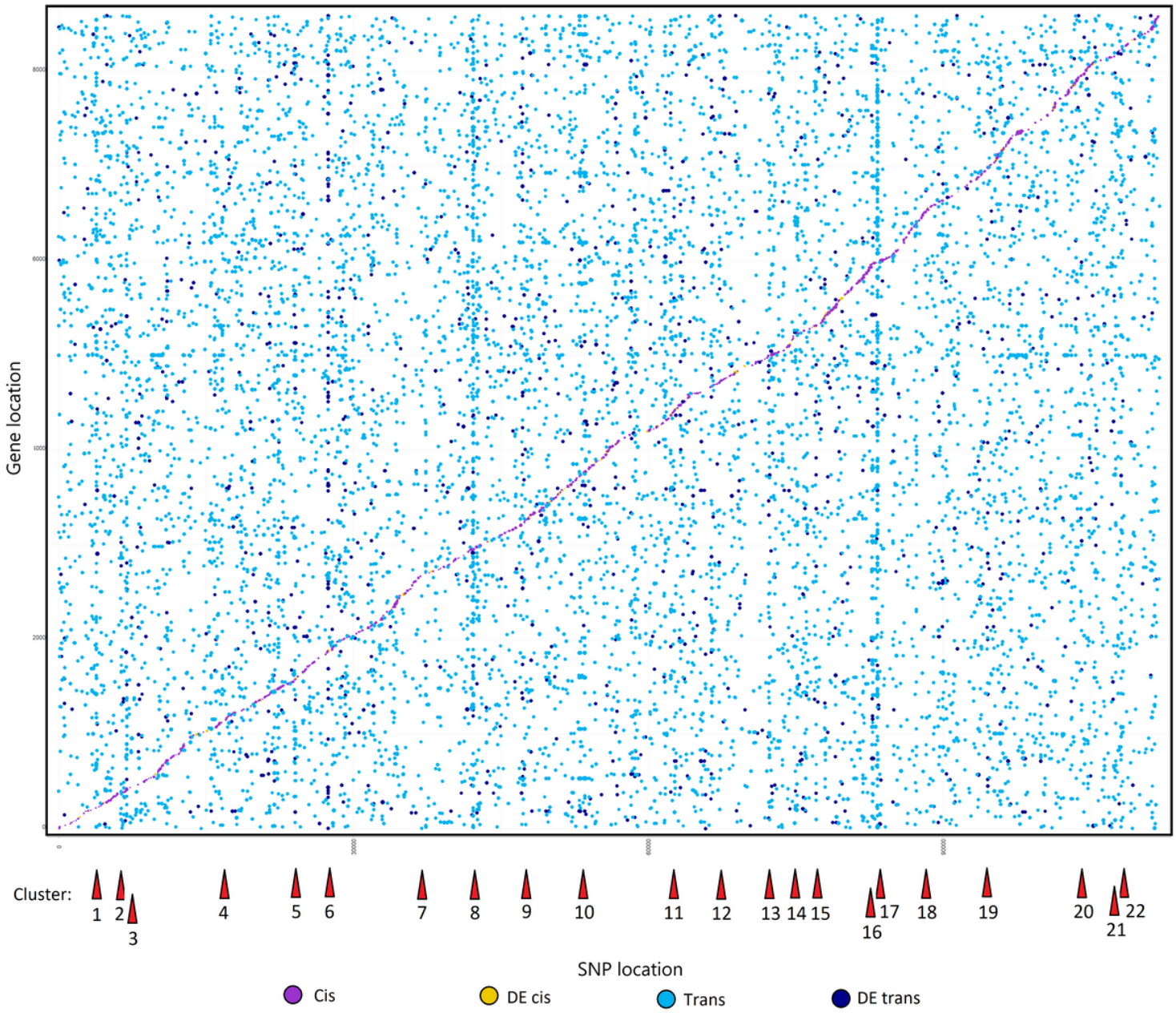

Figure 1

Expression QTL mapping in longissimus dorsi muscle sampled from a multibreed Angus-Brahman herd. SNP information about 112,042 markers, and expression data from 8,588 genes were included in the association assay. Expression of DE genes was previously identified as related to meat quality traits in the same papulation. A total of 8,377 eQTLs were included. Dot size represent significance level for each association test. Red triangles locate each cluster of hot spots. Hot spots are described in more detail in Table 1.

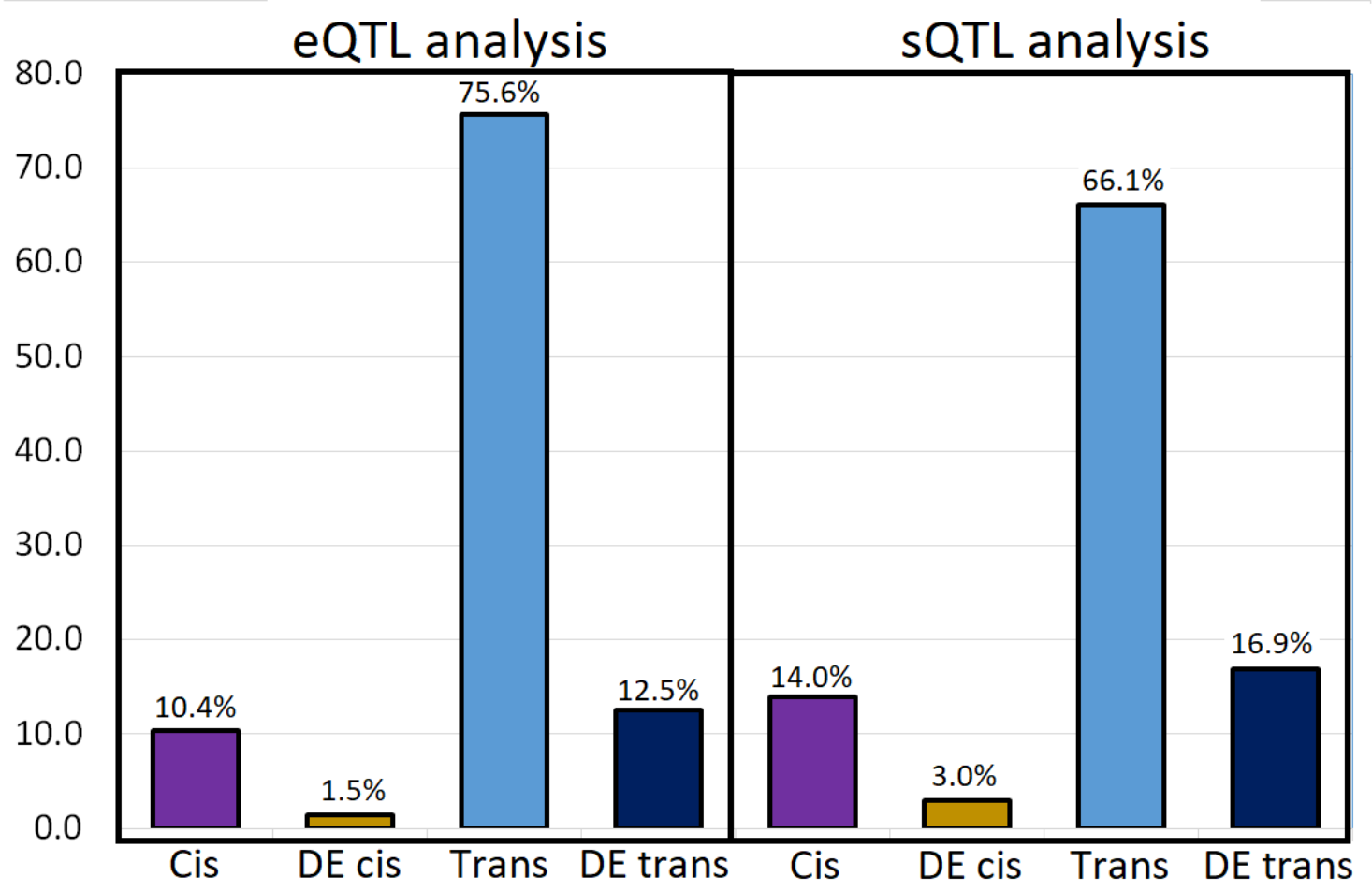

Figure 2

Frequency of each type of eQTL and sQTL identified. The QTL mapping analysis was performed in longissimus dorsi muscle sampled from a multibreed Angus-Brahman herd.

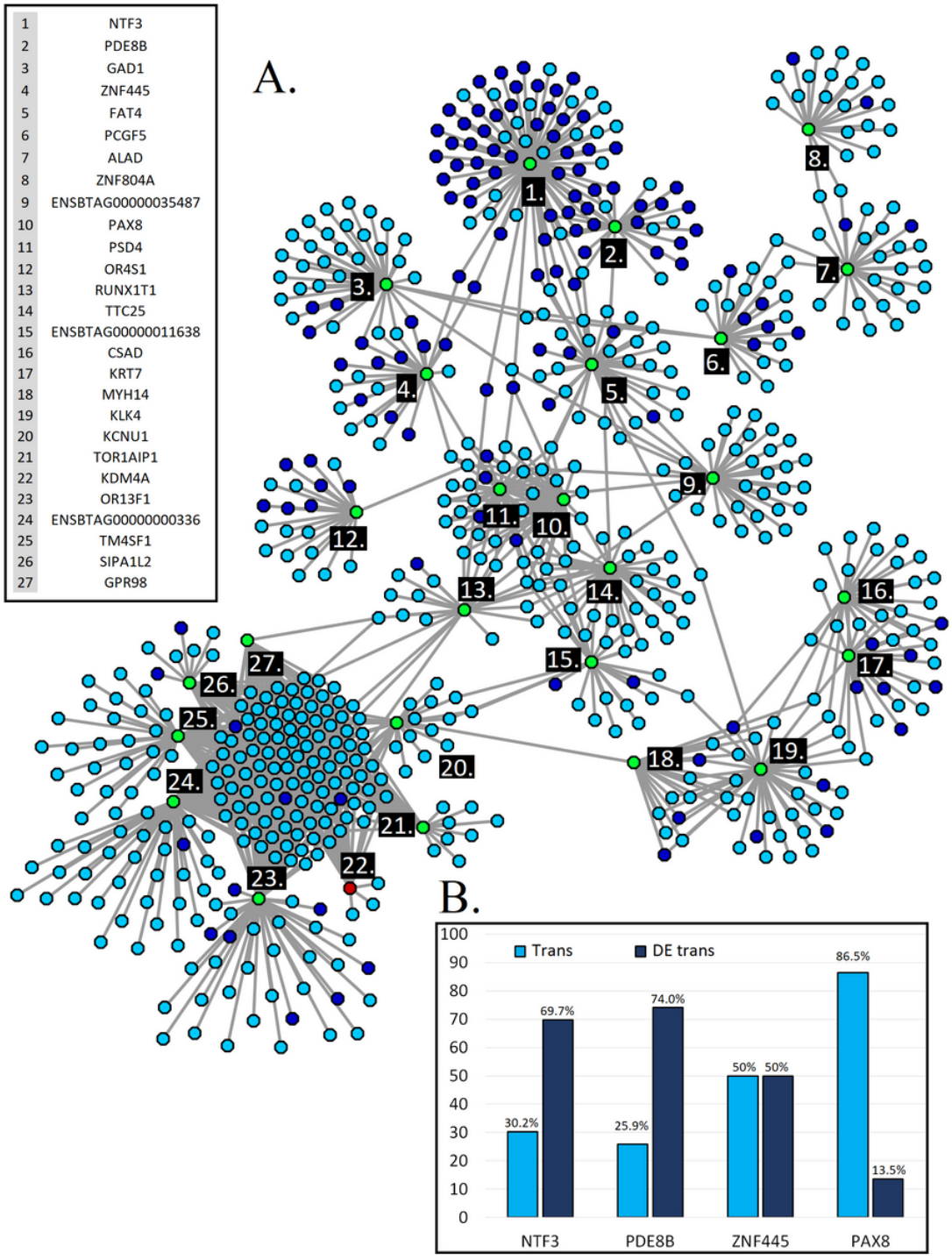

Figure 3

Network for 27 expression master regulators and 674 regulated genes identified using eQTL mapping. Green = Master regulator; red = DE master regulator; light blue = Regulated gene; dark blue = DE regulated gene; 3B. Percentage of trans and DE trans regulated genes in the clusters NTF3, PDE8B, ZNF445 and PAX8.

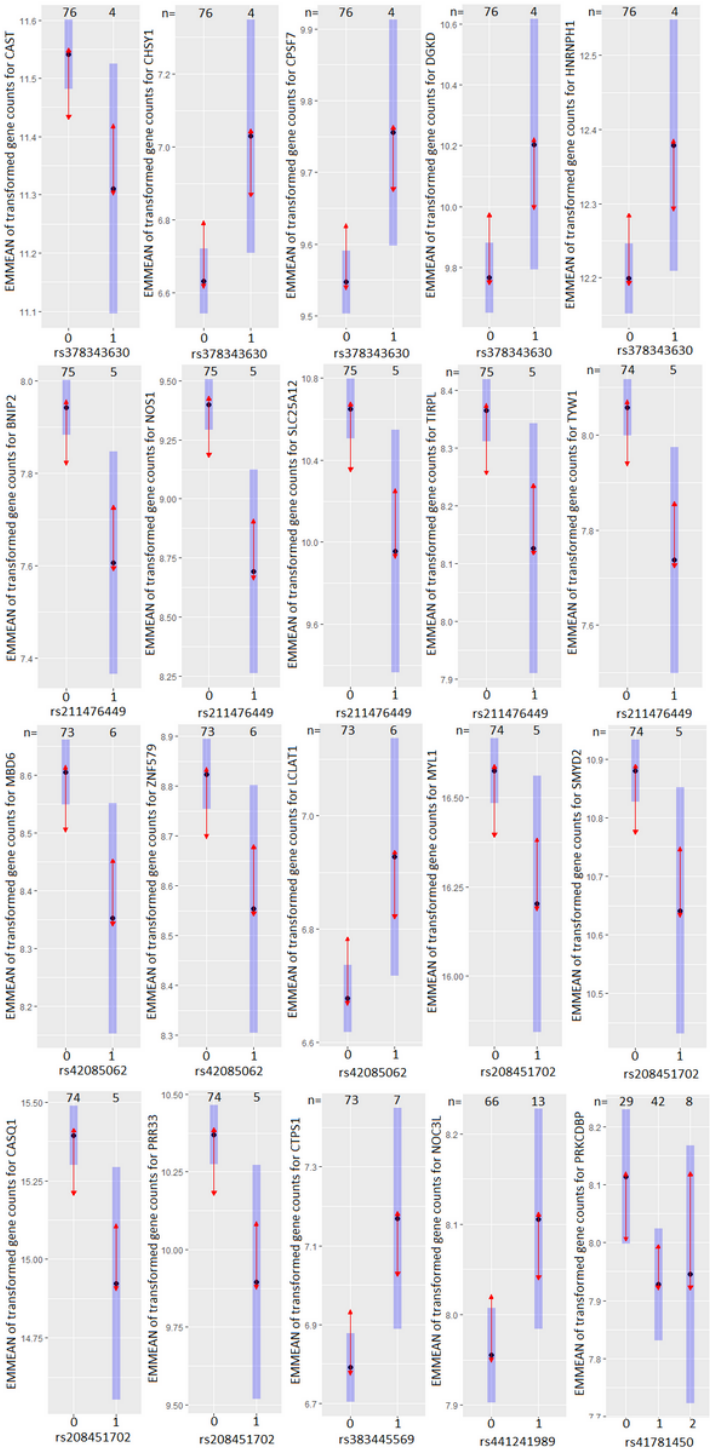

Figure 4

Least-square mean plots for SNP effect on transformed gene counts of some regulated genes for the master regulators TM4SF1 (rs378343630), GAD1 (rs211476449), PCGF5 (rs42085062), RUNX1T1 (rs208451702), KLK4 (rs383445569), CSAD (rs441241989) and OR4S1 (rs41781450). The eQTL mapping was performed in longissimus dorsi muscle sampled from a multibreed Angus-Brahman herd.

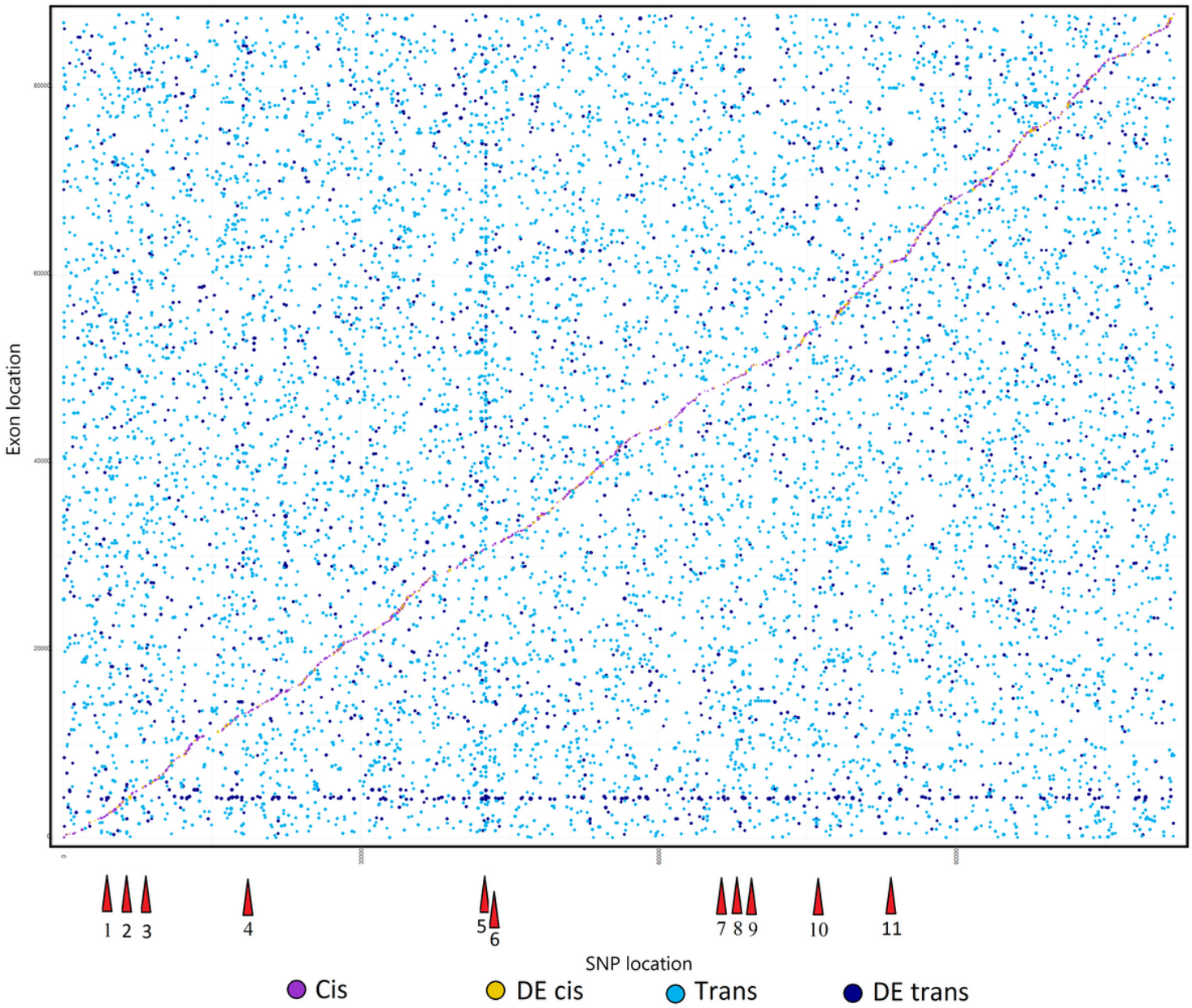

Figure 5

Splicing QTL mapping in longissimus dorsi muscle sampled from a multibreed Angus-Brahman herd. SNP information about 112,042 markers, and expression data from 87,770 exons (8,467 genes) were included in the association assay. DE genes were previously identified as related to meat quality traits in the same papulation. A total of 11,929 sQTLs were included. Dot size represent significance level for each association test. Red triangles locate shows the location of one or several hot spots. Hot spots are described in more detail in Table 3.

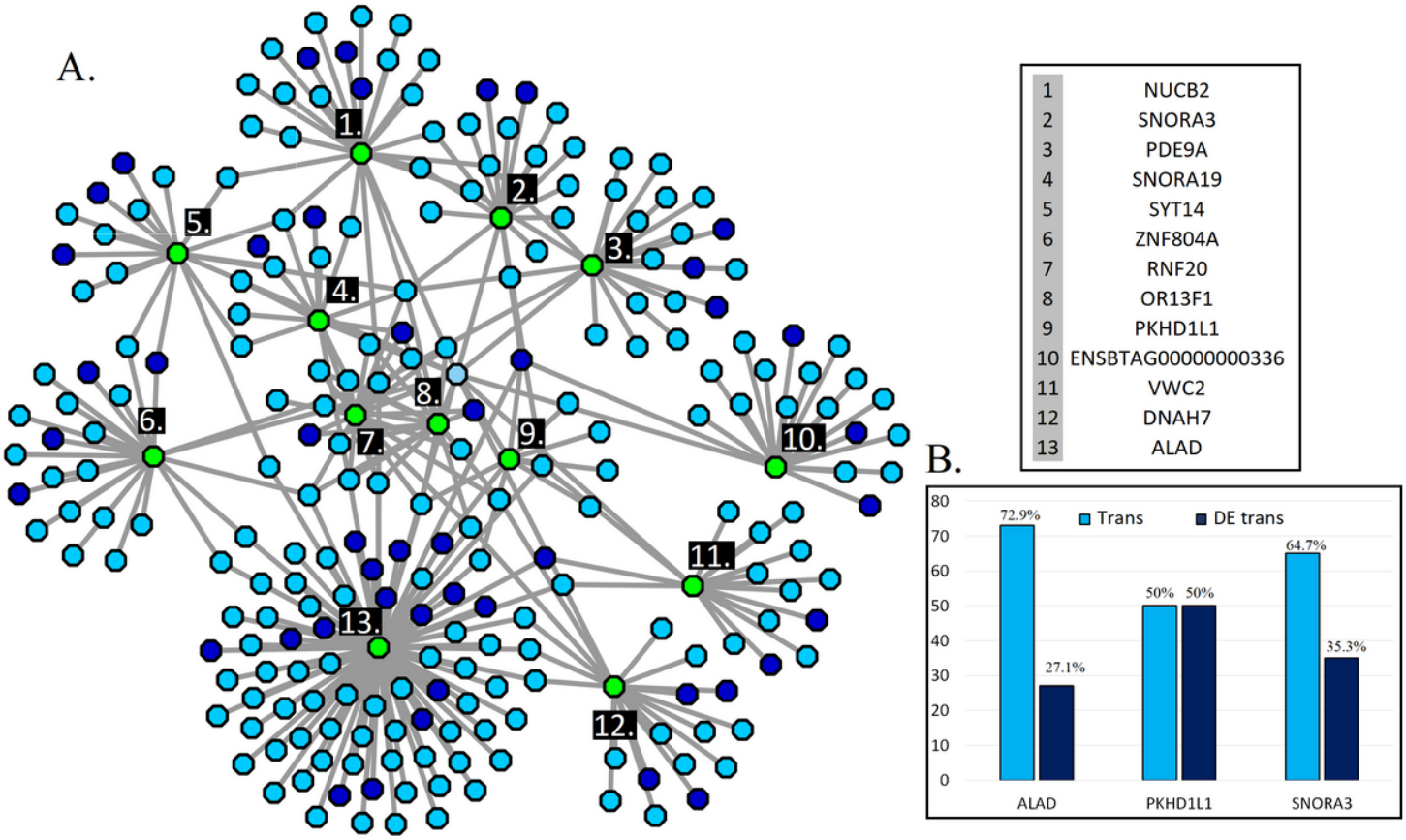

Figure 6

Network for 13 splicing master regulators and 231 regulated genes identified using sQTL mapping. Green = master regulator; light blue = regulated gene; dark blue = DE regulated gene; 6B. Percentage of trans and DE trans regulated genes in the clusters ALAD, PKHD1L1 and SNORA3.

Supplementary Files

This is a list of supplementary files associated with this preprint. Click to download.

- BMCArrivalFormatGICSD1901098.xlsx
- eq1.jpg
- Additionalfile1.xlsx
- Additionalfile5.xls
- Additionalfile3.xls
- Additionalfile4.xls
- Additionalfile6.xlsx
- Additionalfile2.xls